

Improvement of Fatigue Strength of Welded Joints by Grain Refinement Using Laser Irradiation and Locally Carburized

TERATSUJI, Kazutaka

Department of Naval Architecture and Ocean Engineering, Graduate School of Engineering, Kyushu University : Master course student

UCHIMURA, Tomoya

Technical Division, School of Engineering, Kyushu University : Technician

MATSUDA, Kazuki

Department of Marine Systems Engineering, Faculty of Engineering, Kyushu University : Associate Professor

GOTOH, Koji

Department of Marine Systems Engineering, Faculty of Engineering, Kyushu University : Professor

<https://hdl.handle.net/2324/7157262>

出版情報 : Proceedings of The 36th Asian-Pacific Technical Exchange and Advisory Meeting on Marine Structures (TEAM 2023), pp.63-70, 2023-10-12

バージョン :

権利関係 : Copyright by Authors of Presentation



Improvement of Fatigue Strength of Welded Joints by Grain Refinement Using Laser Irradiation and Locally Carburized

Kazutaka TERATSUJI^{*1}, Tomoya UCHIMURA², Kazuki MATSUDA³, Koji GOTOH⁴

1) Master course student, Department of Naval Architecture and Ocean Engineering, Graduate School of Engineering, Kyushu University; 744, Motooka, Nishi-ku, Fukuoka, 819-0395, Japan
e-mail: teratsuji.kazutaka.950@s.kyushu-u.ac.jp

2) Technician, Technical Division, School of Engineering, Kyushu University; 744, Motooka, Nishi-ku, Fukuoka, 819-0395, Japan
e-mail: uchimura.tomoya.644@m.kyushu-u.ac.jp

3) Associate Professor, Department of Marine Systems Engineering, Faculty of Engineering, Kyushu University; 744, Motooka, Nishi-ku, Fukuoka, 819-0395, Japan
e-mail: matsuda.kazuki.809@m.kyushu-u.ac.jp

4) Professor, Department of Marine Systems Engineering, Faculty of Engineering, Kyushu University; 744, Motooka, Nishi-ku, Fukuoka, 819-0395, Japan
e-mail: gotoh.koji.481@m.kyushu-u.ac.jp

Abstract

The purpose of this paper is to confirm fatigue strength of welded joints can be improved by grain refinement using laser irradiation and localized carburization considering corrosion and abrasion.

The measured temperature histories due to laser irradiation were compared with theoretical solutions for moving and instantaneous line heat sources, and it was confirmed that the temperature history could be estimated well using moving heat source. Maximum temperature and time required from 800 °C to 500 °C ($\Delta t_{8/5}$) of the grain refinement region are obtained by applying moving heat source.

Four-point bending fatigue tests were conducted on T-joint specimens as welded, laser irradiated, and locally carburized. As a result, number of cycles to failure of the specimens which locally carburized and laser irradiated were equivalent and they are longer than that of the specimens as-welded. The main reason is locally carburized and laser irradiated had more gentler toe shapes than as-welded. However, the porosity was observed in the carburized specimen. It can affect fatigue strength, further improvement of fatigue strength was expected by eliminating it.

Keyword: Laser irradiation, Grain refinement, Local carburizing, Fatigue strength of welded joint

1. INTRODUCTION

Large scale welded structures, such as ships and offshore structures are mostly failed by fatigue loading. Especially, fatigue cracks tend to generate from stress concentration regions, such as weld toes. Many studies such as HFMI, have been conducted to address these fatigue strength issues. However, most of the secondary processing for fatigue life improvement is done manually after welding, which is disadvantageous in terms of construction cost and time, taking into account that the weld length of ships is sometimes over 500 km. On the other hand, some of the authors have shown that laser irradiation of weld toe under appropriate conditions during the fabrication process of welded joints can simultaneously relieve stress concentration, grain refinement and localized carburization, and these results are expected to significantly improve fatigue life of the joints.

It is known that local laser irradiation of the steel surface layer causes a local temperature change across the phase transformation temperature during the process of local heating and subsequent cooling, and this effect results in grain refinement of surface layer [1].

Although grain refinement improves strength and suppresses fatigue crack initiation, there is a concern that corrosion and wear due to degradation might cause the surface refinement layer to disappear, resulting in a loss of fatigue strength improvement effect. Considering that in hull structures, corrosion additions of 1 mm is required for members exposed to sea water and 1.0 to 5.2 mm for dry bulk hold [2], the imposition of grain refinement effects to some depth from the plate surface is considered necessary.

Various studies have been conducted on grain refinement by laser irradiation. However, there is no study changing conditions of laser power, travel speed and defocus distance. The objective of this paper is to improve fatigue strength

of welded joints by simultaneously achieving grain refinement at deeper depths to deal with corrosion addition and localized carburization at the surface layer of weld toe in a single laser irradiation.

2. COMPARISONS WITH THEORETICAL SOLUTIONS AND MEASURED VALUE ON TEMPERATURE HISTORY

2.1. Influence investigation of defocus distance

In terms of metallurgy, condition range of temperature history, such as the peak temperature and the cooling time from 800 °C to 500 °C ($\Delta t_{8/5}$), need to be clear to control grain refinement. If theoretical solutions and measured value are matched, arbitrary position of temperature history can be obtained. Therefore, laser irradiation conditions which can apply theoretical solutions were investigated. Laser irradiation conditions is listed in **Table 1**.

Mild steel (Class NK standard, grades KA and KA36) are applied in this study. The standard carbon steel values [3] shown in **Table 2** were used as physical properties in this study. Temperature histories on the five points shown in **Fig. 1** were measured and compared with theoretical solutions based on moving heat source (1) and instantaneous line heat source (2) [4]. η of theoretical solution is adjusted to match maximum temperature of CH 1. **Figure 2** compares the theoretical solutions with the measured values. **Table 3** shows the thermal efficiency η of theoretical solution. **Figure 3** shows cross-sectional observation of molten and heat affected zone by laser irradiation. **Figure 4** shows examples of the estimated temperature distribution near the laser irradiated zone based on theoretical solutions. According to **Fig. 2**, only moving heat source matched measured value when the defocus distance of laser beam (D.D.) is 25 mm to some extent. On the other hand, both of temperature histories of theoretical solutions are lower than those of measured value when D.D. is 5 mm. **Figure 3** shows that fusion zone is deep and narrow when D.D. is 5 mm, while the fusion zone is nearly a semicircle when D.D. is 25 mm. **Figure 4** shows that the fusion zone shapes estimated by the theoretical solution based on moving and instantaneous line heat sources are semicircular. From these results, it can be confirmed that a large differences in the temperature history between the theoretical solutions and measured values occurs when the estimation accuracy of the fusion zone shape is poor. As a result of comprehensively considering the situations described above, the D.D. at 25 mm is applied in the subsequent study.

Table 1 Laser irradiation conditions.

Speciman ID.	Laser power [kW]	Travel speed [mm/min]	Defocus distance (D.D.) [mm]	Plate thickness [mm]	Steel grade
A	3.0	500	+5	12	KA
B			+25		

Table 2 Property of applied mild steel.

Density [g/cm ³]	Specific heat [J/kg °C]	Thermal conductivity [W/m K]
7.83	461	53

$$\theta = \left(\frac{\eta q}{2\pi\lambda} \right) \cdot \sum_{n=0}^{\infty} \frac{\exp \left[\left\{ -v\rho C(x + \sqrt{x^2 + y^2 + (z \pm 2nh)^2}) \right\} / 2\lambda \right]}{\sqrt{x^2 + y^2 + (z \pm 2nh)^2}} + \theta_p \quad (1)$$

$$\theta = \left(\frac{\eta q}{2\pi v \lambda t} \right) \cdot \sum_{n=0}^{\infty} \exp[-\rho C \{y^2 + (z \pm 2nh)^2\} / 4\lambda t] + \theta_p \quad (2)$$

θ : Temperature [°C], η : Thermal efficiency, q : Laser power [W], v : Travel speed [cm/s], ρ : Density [g/cm³], C : Specific heat [J/kg °C], λ : Thermal conductivity [W/cm K], θ_p : Initial temperature [°C]

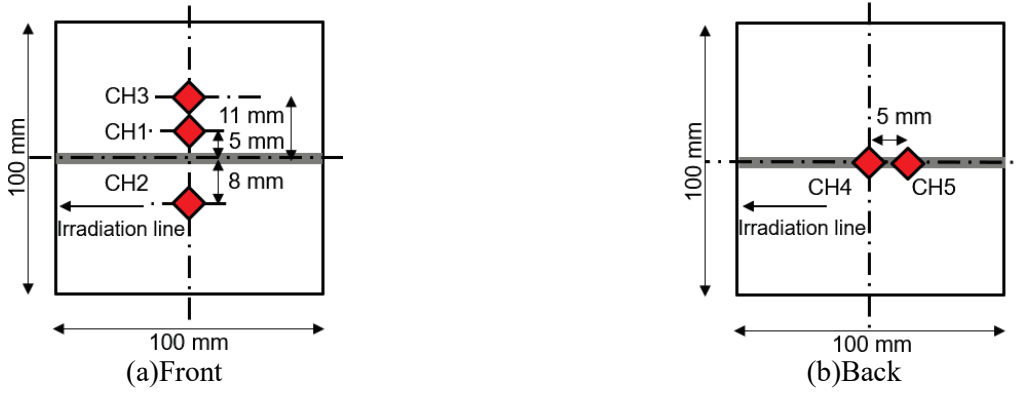


Fig. 1 Temperature history measuring points.

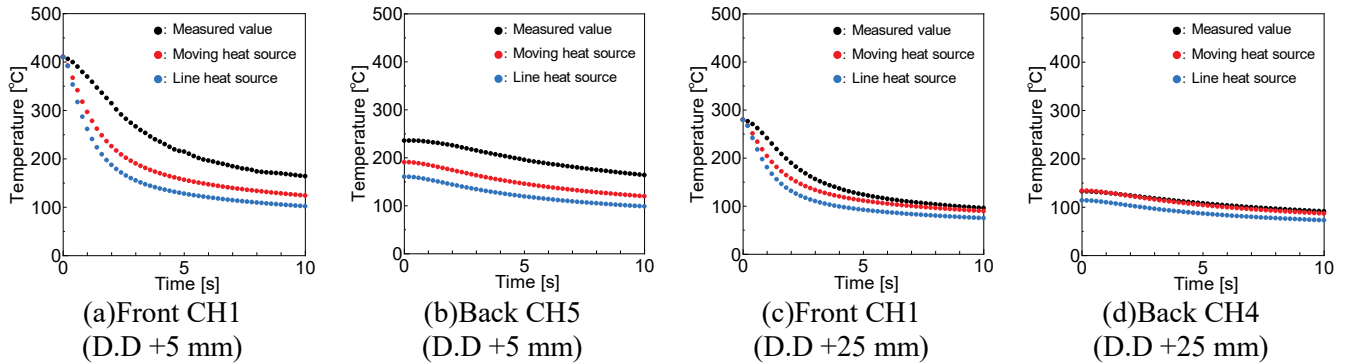
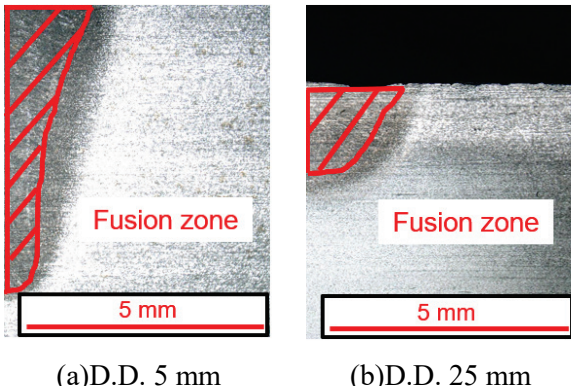


Fig. 2 Comparison of measured temperature history with theoretical solution.

Table 3 Thermal efficiency of theoretical solution.

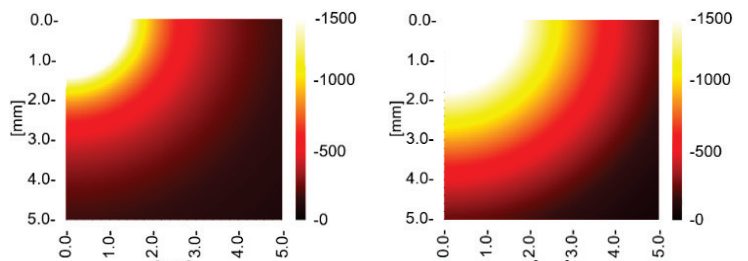
Defocus distance : D.D.	Moving heat source	Instantaneous line heat source
5 mm	0.5394	0.4107
25 mm	0.3576	0.2723



(a) D.D. 5 mm

(b) D.D. 25 mm

Fig. 3 Cross-sectional observations.



(a) Moving heat source

(b) Instantaneous line heat source

Fig. 4 Temperature distributions in the cross section.

2.2. Influence investigation of laser power, travel speed and plate thickness

The effect of laser power, travel speed and plate thickness on difference between measured values and theoretical solutions were investigated. The laser irradiation conditions are listed in **Table 4**. Test IDs 1 to 9 is set to search the effect of laser power and travel speed. Test IDs 10 and 11 is set to search the effect of plate thickness. The width of specimen was changed from 100 mm shown in **Fig. 1** to 150 mm. **Figures 5 to 7** show a part of the comparison with measured value and theoretical solutions. The temperature measured positions were the same mentioned in section 2.1. **Figure 5** shows that the estimated temperature distribution based on moving heat source are closer to the measured values than those based on instantaneous line heat source. As for the comparison between theoretical solutions based on the instantaneous line heat source and measured values, the result were similar to those shown in section 2.1 when travel speed was 500 mm/min, but the results agreed to some extent when travel speed was over 750

mm/min. **Figures 6** and **7** shows a comparison of the temperature distributions from the theoretical solutions with measured ones for different of plate thickness. For a plate thickness of 8 mm, both theoretical values are larger than the measured values on the back surface. The reason why is assumed to be that the theoretical solution treats the heat reflection on the back surface of the plate as adiabatic and does not reflect the relatively large effect of dissipation of part of heat input by radiation. Based on these results, the condition under which the theoretical solution can correctly estimate temperature is a thickness of 12 mm or greater.

Table 4 Laser irradiation conditions.

Test ID	Laser power [kW]	Travel speed [mm/min]	Plate thickness [mm]	Steel grade	
1	1.0	500	12.5	KA36	
2		750			
3		1,000			
4	3.0	500	12.5		
5		750			
6		1,000			
7	5.0	500	8.0		
8		750			
9		1,000			
10	3.0	750	20		
11					

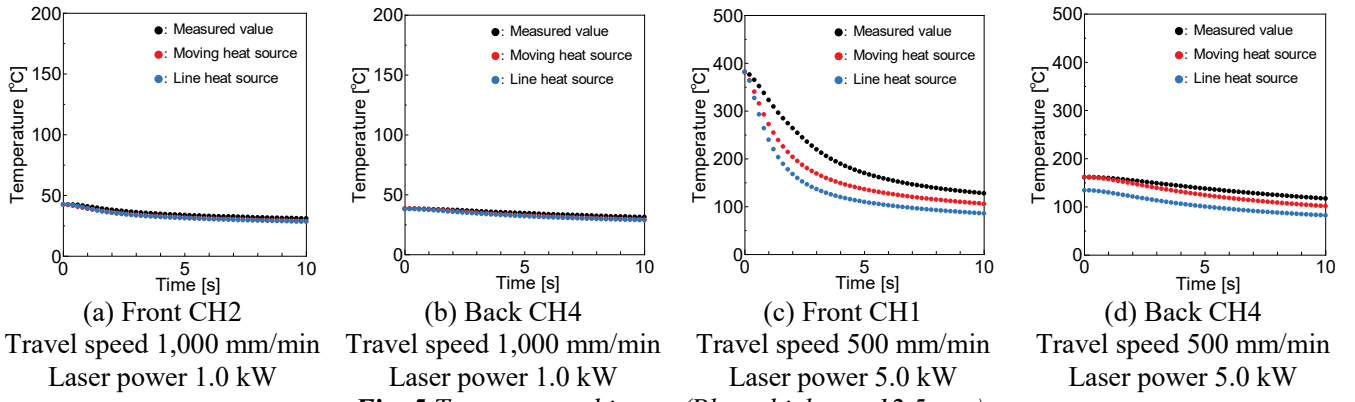


Fig. 5 Temperature history (Plate thickness 12.5 mm).

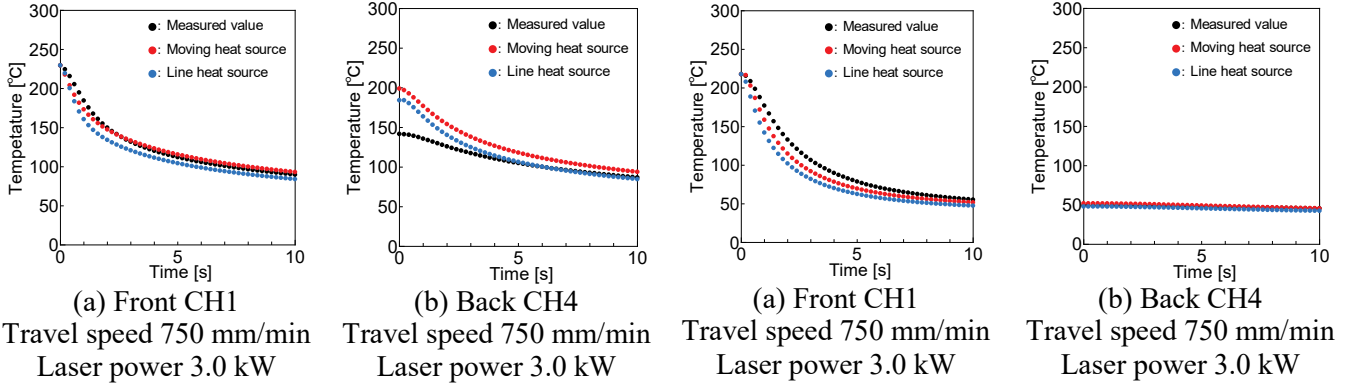


Fig. 6 Temperature history
(Plate thickness 8.0 mm).

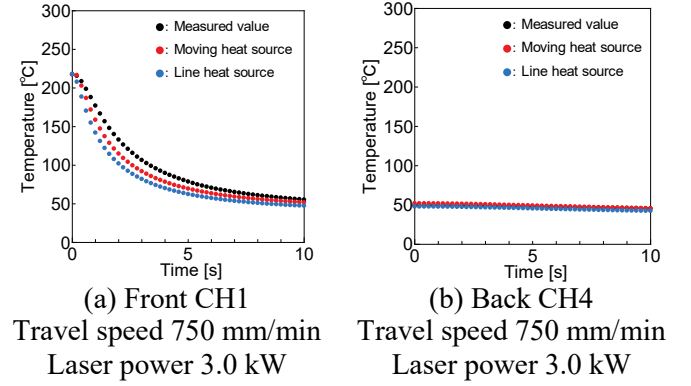


Fig. 7 Temperature history
(Plate thickness 20 mm).

3. OCCURRENCE CONDITION OF GRAIN REFINEMENT

Considering maximum temperature and cooling time from 800 °C to 500 °C ($\Delta t_{8/5}$) influence on maximum hardness and grain diameter, it is expected that there is some relationship between grain refinement condition and $\Delta t_{8/5}$. After observing the specimen with D.D. of 25 mm shown in section 2.1 and measuring the depth of the grain refinement layer, the temperature history at the location of grain refinement layer was determined. The center fusion zone on the surface of specimen was set as the origin, and grain refinement layer was defined as the one whose grain size is

smaller than that of base metal. **Figure 8** shows the metallographic structure of the base metal. **Figure 9** shows the metallographic structure structure including grain refinement layer. The grain diameter was measured in accordance with Japanese industrial standards JIS G 0551 [5]. The grain refinement layer was located from 2.18 mm to 2.35 mm at deepest point in the laser travel direction. **Figure 10** shows the temperature history of grain refinement layer, by applying the theoretical solution based on moving heat source. The maximum temperature and $\Delta t_{8/5}$ of grain refinement layer near fusion zone were 930 °C and 0.384 s, respectively. On the other hand, the maximum temperature and $\Delta t_{8/5}$ of grain refinement layer near the base metal were 839 °C and 0.424 s, respectively. Therefore, occurrence of grain refinement is the maximum temperature need to be between 839 °C and 930 °C and $\Delta t_{8/5}$ need to be between 0.384 s and 0.424 s. Considering that the A₃ point of general steel is around 900 °C, the thermal cycle that the grain refinement layer underwent is considered reasonable.

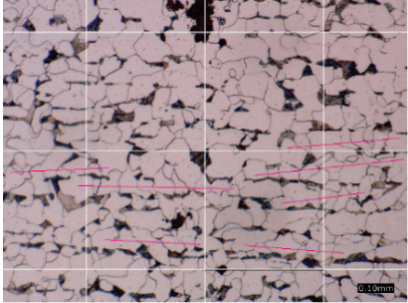


Fig. 8 Base metal's crystal grain.

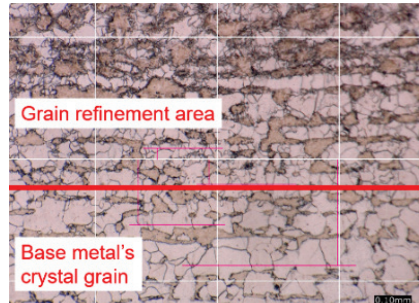


Fig. 9 Grain refinement area and base metal's crystal grain.

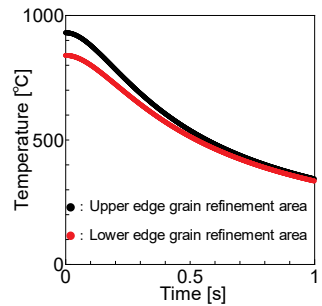


Fig. 10 Temperature histories of grain refinement area solved by theoretical formula of moving heat source.

4. FOUR-POINT BENDING FATIGUE TEST

Four-point bending fatigue tests were conducted to investigate the effect of laser irradiation on grain refinement and local carburization at the weld toe on fatigue life. T-shaped joints were applied as the welded joints to be evaluated, and three types of specimen were prepared: one with only laser irradiation at the weld toe, one with local carburizing treatment at weld toe, one without laser irradiation as a comparison. Fabrication condition of T-shaped joint is shown in **Table 5** and **Fig. 11** [6]. Applied steel is mild steel of grade KA by ClassNK with thickness 12 mm. **Figure 12** and **Table 6** show laser irradiation location and condition that have been explored as appropriate conditions in previous study [7]. The fatigue test were planned from two perspectives. The first is a comparison of fatigue strength improvement between laser irradiation only and local carburization. The second is a comparison of joints in which only laser irradiation was performed, but with varying conditions in order to change the degree of grain refinement. To aid in the discussion of the test results, the geometry of weld toe shape was measured with a laser scanner and residual stresses were measured subsequently by X-ray diffraction. **Figure 13** shows definition of shape of welded toe. **Figure 14** shows the specimen dimensions and **Fig. 15** shows load and support points under loading. They were set up in accordance with ISO 12018 [8]. In addition, a preliminary specimens were used to measure the Vickers hardness in the laser irradiation region. Measured location is shown in **Fig. 16**. Fatigue tests were conducted in accordance with ISO/TR 14345 [9]. Applied stress ranges were 275, 300, 350 and 400 MPa in stress ratio 0.1 and 10 Hz in cyclic frequency. The results of fatigue test tests are shown in **Fig. 17**. The number of cycles to failure of the specimens which locally carburized and laser irradiated were equivalent and they are longer than that of the specimens as-welded. On the other hand, the effect of different laser irradiation travel speed on the improved fatigue strength was unclear. **Figures 18** and **19** show the distributions of measured residual stress and Vickers hardness. **Figures 20 to 25** shows shape of welded toe. The results shown in **Fig. 18** indicate that the residual stresses in all the specimens are approximately the same. **Figure 19** shows that the hardness of locally carburized specimen exceeds 900 HV because of carbon penetration. The hardness of fast laser-irradiated (ID.5) is harder than that of slow laser-irradiated (ID.4). Hardness of laser-irradiated (ID.3) and as-welded are equivalent. According to **Figs. 20 to 25**, the flank angle, toe radius and stress concentration factor obtained by equations (3) through (6) [10] of weld toe treatment were improved. Based on a comprehensive analysis of the above results, it is considered that the main reason for the improvement in fatigue strength of the joints to which only laser irradiation in this fatigue test is the reduction of stress concentration

due to the relaxation of the weld toe geometry. In addition to the relaxation of the weld toe shape, the localized carburizing joints were significantly hardened at the weld toe as shown in **Fig. 19**, which suppressed crack initiation. On the other hand, as illustrated in **Fig. 26**, the presence of porosity was observed in the local carburized area. Although the location of crack initiation in the locally carburized joint was not confirmed in detail, the possibility that fatigue cracks were generated from porosity cannot be denied. From another viewpoint, the fatigue strength is expected to be further improved by optimizing the local carburizing conditions and eliminating porosity.

Table 5 Arc welding conditions.

Arc current [A]	Arc voltage [V]	Travel speed [cm/min]	Distance of wire aiming point [mm]	Torch direction angle [deg.]	Torch elevation angle [deg.]	wire Extension [mm]	Gass mass flow [L/min]	Wire diameter [mm]
220	26	38	0	0	40	20	20	1.4

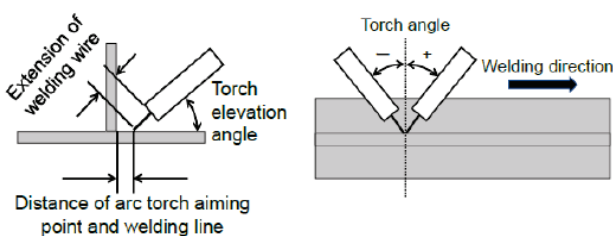


Fig. 11 Definition of arc welding.

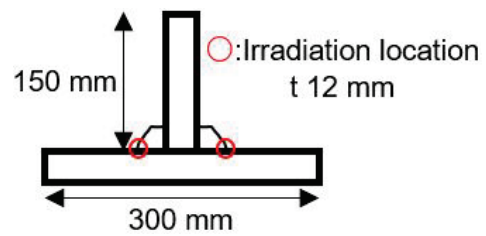


Fig. 12 Irradiation location.

Table 6 Laser irradiation conditions.

ID.	Laser power [kW]	Defocus distance [mm]	Travel speed [mm/min]	Formulation of paste (C:Si:H ₂ O)	Thickness of paste [mm]	Laser angle [deg]
1	None (As-welded)	None	None	None	None	None
2	1.5	-5	120	10:20:14	0.5	45
3				None	None	
4	3.0	+25	500			45
5			1,000			

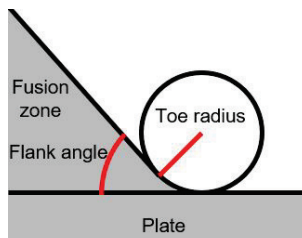


Fig. 13 Definition of weld toe.

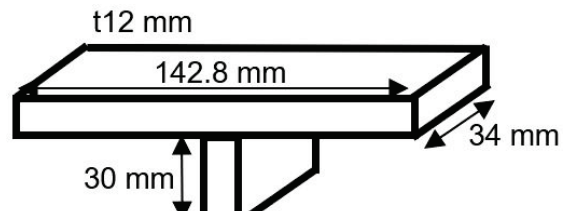


Fig. 14 Size of specimen.

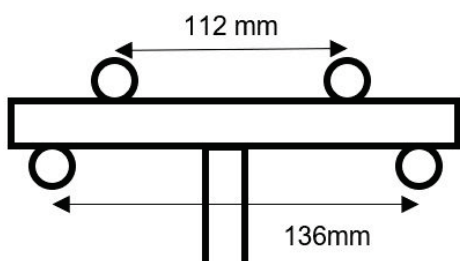


Fig. 15 4-point bending fatigue.

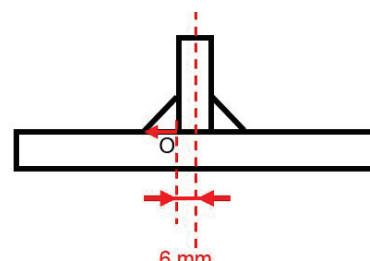


Fig. 16 Origin of Vickers hardness test.

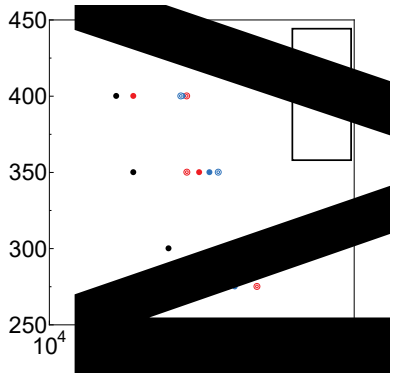


Fig. 17 Result of fatigue test.

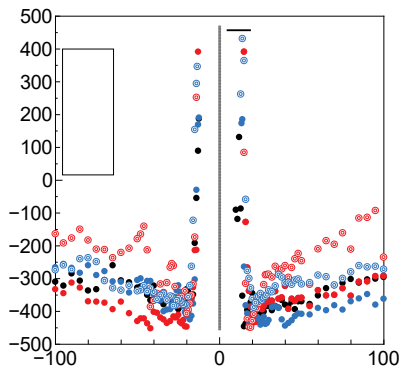


Fig. 18 Measurement of residual stress.

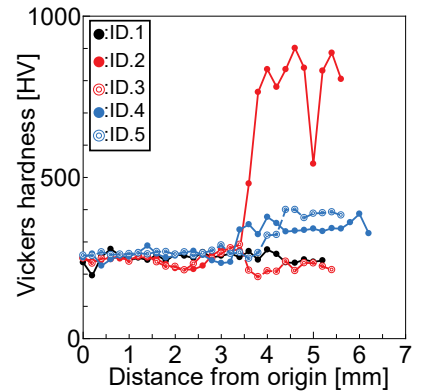


Fig. 19 Measurement of Vickers hardness.

$$K_t = 1 + \left\{ 0.629 + 0.058 \cdot \ln \left(\frac{S}{t} \right) \right\} \cdot \left(\frac{\rho}{t} \right)^{-0.431} \cdot \tanh \left(\frac{6h}{t} \right) \cdot f_\theta \quad (3)$$

$$f_\theta = \frac{1 - \exp \left\{ -0.90 \sqrt{\frac{W}{2h}} \cdot \theta \right\}}{1 - \exp \left\{ -0.90 \sqrt{\frac{W}{2h}} \cdot \frac{\pi}{2} \right\}} \quad (4)$$

$$W = t + h \quad (5)$$

$$S = t_p + 2h_p \quad (6)$$

K_t : Stress concentration factor, t : thickness of main plate, t_p : thickness of vertical plate,

h : Leg length of vertical plate, h_p : Leg length of main plate side, θ : Flank angle, ρ : weld toe radius.

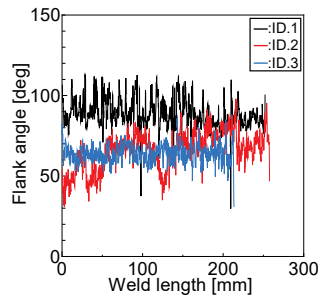


Fig. 20 Flank angle (No.1).

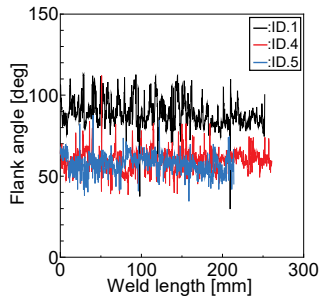


Fig. 21 Flank angle (No.2).

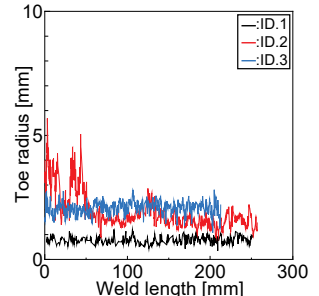


Fig. 22 Weld toe radius (No.1).

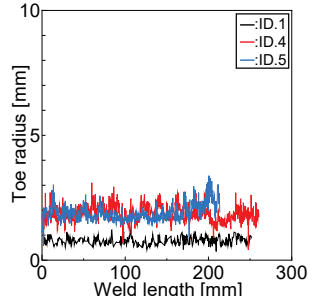


Fig. 23 Weld toe radius (No.2).

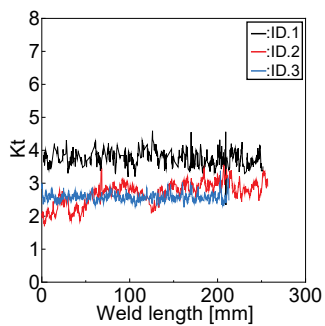


Fig. 24 Stress concentration factor K_t (No.1).

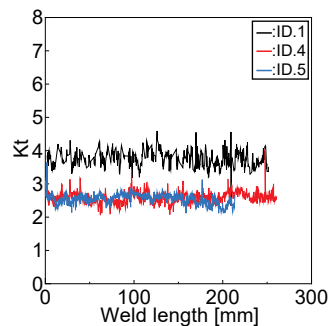


Fig. 25 Stress concentration factor K_t (No.2).

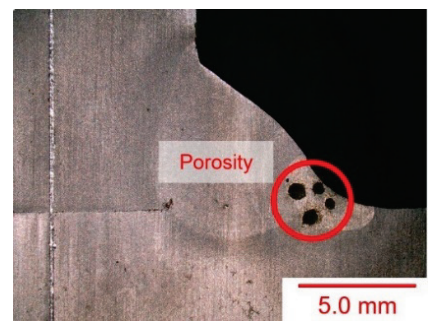


Fig. 26 Porosity in locally carburized zone.

5. CONCLUSIONS

In this study, it is purpose to control grain refinement and make localized carburized zone in the pointview of fatigue strength and corrosion addition. Comparisons with theoretical solutions and measured value on temperature history, occurrence condition of grain refinement and four-point bending fatigue test are investigated.

The conclusions are as follows:

- (1) Moving heat source matched measured value when defocus distance was 25 mm from the front surface of plate.
- (2) Occurrence condition (maximum temperature and $\Delta t_{8/5}$) of grain refinement was investigated, by applying moving heat source and observing crystal grain.
- (3) Stress concentration was relieved by laser irradiation near the weld toe, and fatigue strength was improved.
- (4) Fatigue strength could be further improved by eliminating porosity in localized carburized zone.

ACKNOWLEDGEMENTS

We would also like to express our sincere thanks to Professor Yasuhiro MORIZONO, Department of Materials System Engineering, National Institute of Technology, Kurume College, for guiding the method of micro observation and constructive suggestions for this research. In addition, we would thank to Koji MURAKAMI, Technical Division, School of Engineering, Kyushu University, for his cooperation of experiments.

This work was supported by JSPS Grant-in-Aid for Scientific Research (B), Grant Number JP 20H02372.

REFERENCES

- [1] Nisio, K., Katoh, M. and Yamaguchi, T., Grain Refinement by Laser Irradaiton, Function & Materials, Vol.27, No.7, 2007, pp.56-60. (in Japanese)
- [2] Nippon Kaiji Kyokai (ClassNK): Rules for the Survey and Construction of Steel Ships Contents Part CSR-B Common Structural Rules for Bulk Carriers, (2015).
- [3] <https://www.hakko.co.jp/qa/qakit/html/h01020.htm>, accessed on Jan 26, 2023
- [4] Terasaki, T. et al.: Prediction of Cooling Time for Ferrite-Austenite Transformation in Duplex Stainless Steel, ISIJ International, Vol. 35, No.10, pp.1272-1276, (1995).
- [5] Japan Industrial Standards JIS G 0551, Steel-Micrographic determination of the apparent grain size, (2022).
- [6] Feng, Y. et al.: Fundamental Study on Prediction of GMAW Bead Shapes Based on Deep Learning Using of Welding Conditions and Arc Sound Features, Journal of The Japan Welding Society, Vol. 19, pp.41-44. (in Japanese)
- [7] Tamon, T. et al.: Basic Research on Local Carburizing Treatment by Laser Irradiation for Fatigue Strength Improvement of Welded Joints, Journal of The Japan Society of Naval Architects and Ocean Engineers, Vol 34, pp.467-472. (in Japanese)
- [8] ISO 12108, Metallic materials-Fatigue testing-Fatigue crack growth method, (2002)
- [9] ISO/TR 14345 Fatigue-Fatigue testing of welded components-Guidance, (2012)
- [10] Tsuji, I: Estimation of stress concentration factor at weld toe of non-load carrying fillet welded joints, Journal of The Japan Society of Naval Architects and Ocean Engineers, Vol 80, pp.241-251. (in Japanese)